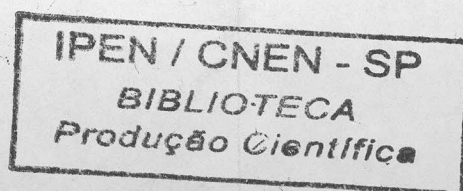


Hyperfine Magnetic Fields in the Cobalt based Heusler Alloys:
A Systematic Investigation Using PAC

R.N. Saxena

Invited Talk

25th Anniversary of Hyperfine Interactions at La Plata
March 27 to 31, 1995
La Plata, Argentina



5109

HYPERFINE MAGNETIC FIELD

- Imagine an atomic nucleus implanted in a ferromagnetic host material such as Fe. Interaction between the nucleus and spin polarized electrons in the host lead to an effective magnetic field which is commonly called “hyperfine field” H_{hf} .
- This hyperfine field provides microscopic information on the electronic state of the host and has been investigated extensively especially in 3d-transition ferromagnets like Fe, Co and Ni.
- It is well known that H_{hf} in a given 3d-ferromagnet shows oscillatory behavior as a function of z-number of the impurity atom. Hyperfine field is negative (in opposite direction to the host magnetization) for d- transition atoms and at the beginning of the s-p series, crosses zero at the middle of each s-p series and becomes large and positive at the end of the series.

- In the region where H_{hf} crosses zero, one might expect that the net field is the sum of two large contributions with opposite signs and the net field will be very sensitive to the delicate balance of these two competing contributions.
- Direct information on the individual components is very difficult to obtain experimentally. It is therefore essential to obtain a large amount of information on a variety of magnetic systems apart from the traditional ferromagnets like Fe, Co, Ni, Gd etc.

ORIGIN OF HYPERFINE MAGNETIC FIELDS

- The hyperfine field H_{hf} is the magnetic field seen by the nucleus with a magnetic moment (μ). The interaction energy is given by

$$E_{hf} = -\vec{\mu} \cdot H_{hf}$$

H_{hf} can be quite a large number, kOe or even MOe (for rare earth nuclei). Different contributions are:

- A. Orbital Angular Momentum (L)

Interaction between the nucleus and the orbital angular momentum of its own electron is given by:

$$E_L = \frac{2\mu_B \vec{L} \cdot \mu}{r^3}$$

or the field is given as:

$$H_L = -\frac{2\mu_B \vec{L}}{r^3}$$

- This field is small in 3-d transition elements where the orbital moment is almost zero (quenched). It is a major contribution in R.E. elements.

- **B. Nuclear Dipole - Electron Dipole Interaction**

$$H_D = -\frac{\vec{\mu}_e}{r^3} + \frac{3(\vec{\mu}_e \cdot \vec{r})\vec{r}}{r^5}$$

μ_e is the electron dipole moment (spin and orbital) if the crystal structure is cubic the dipole-dipole interaction sums up to zero.

- **C. Fermi Contact Interaction**

This is the interaction between the nucleus and an electron at the nuclear site

$$H_{FC} = \frac{-16\pi}{3} \mu_B \langle \sum (s \uparrow - s \downarrow) \rangle$$

$s \uparrow$ and $s \downarrow$ are the s-electron densities at the nucleus with spin up and spin down and μ_B is Bohr magneton.

- **Core s electrons and conduction electrons can contribute to the hyperfine field thru this mechanism. Various mechanisms which can produce finite spin density at the nucleus are:**

i. Core polarization (CP)

Polarization of core s-electrons by the 3d electrons of the same atom: Consider a 3d-magnetic ion like Fe. Inner s electron shells 1s, 2s and 3s are closed. Inner shells therefore should not contribute to the field.

- Calculation by Freeman and Watson (restricted Hartree Fock) show that the coulomb repulsion between s and d- electron is larger when their spins are antiparallel.
- Therefore the spin up $s\uparrow$ electrons are more attracted towards spin up polarised $d\uparrow$ electron relative to spin down $s\downarrow$ electrons resulting in net spin down density at the nucleus. This gives rise to the negative hyperfine field.

ii. Overlap Effect

Transfer of H_{hf} from magnetic to non-magnetic ions:

- Consider a 3d spin up polarized electron on magnetic ion and two electrons one spin up and other spin down occupying s-orbital on a non-magnetic ion and examine the s-electron density at the non-magnetic ion nucleus ($r=0$). This is a three electron problem.

- If $3d\uparrow$, $ns\uparrow$ and $ns\downarrow$ wave functions are mutually orthogonal there is no net spin density on the non-magnetic atom site.
- If however $ns\uparrow$ and $3d\uparrow$ wave functions have finite overlap integral the net effect is to deform the distribution of spin up density so that they stay more on the ion rather than between them. The hyperfine field is therefore always positive.

iii. Covalent effect

In addition to the overlap between $3d\uparrow$ and $ns\uparrow$ let us allow the $ns\downarrow$ electrons to spend some time in the $3d\downarrow$ orbital. This gives rise to positive H_{hf}

iv. RKKY Interaction

Imagine a magnetic ion in the free conduction electron sea. A spin of the conduction electron interacts with the local spin (or the magnetic moment) on the magnetic ion.

- Ruderman and Kittel showed that the localised spin (mag. moment) induces conduction electron polarisation (CEP) which is function of the distance from magnetic ion.

- This polarization has an oscillatory character. The spin density oscillation in the conduction electron sea induced by the magnetic ion gives rise to net spin density at the non-magnetic site. The hyperfine field at the non-magnetic site thus is a function of distance from the magnetic ion and its sign oscillates with distance.
- For 3d transition ferromagnet it gives a negative contribution to H_{hf} at the nearest neighbour distance.

To summarize various contributions:

- i. Orbital angular momentum contribution exists if the impurity is magnetic
- ii. Dipole contribution exists in non cubic hosts.
- iii. The core polarisation contribution is negative and present at magnetic impurity.
- iv. The overlap and covalent effects are present not only in magnetic ions but also in non-magnetic ions. It can be a major contribution to H_{hf} at non-magnetic impurities. Sign of the field is positive.
- v. RKKY interaction contributes to H_{hf} at non-magnetic impurities as well as at magnetic impurities. It is a major contribution for non-magnetic impurities. It's sign depends on the position of the impurity ion relative to the magnetic ion.

SYSTEMATICS OF HYPERFINE FIELDS

- The negative field in the d-transition region is consistent with the core polarization model where inner s-electrons of the impurity are polarized by the local moment of the d-electrons of the same impurity atom.
- On the other hand in the sp-region where the impurity has no magnetic moment the H_{hf} is expected to come only via the conduction electron polarization (CEP) and/or overlap of impurity atom with the host atom.
- Strong dependence on Z-number of the impurity as seen in the wild oscillatory behavior of the systematics of H_{hf} suggest that one can not ignore the local properties around the impurity, such as:

Ionic size, impurity Potencial, local distortion of conduction band, local lattice distortion etc...

- Exact cause of the regular variation of the H_{hf} in sp-region is still not well known.

HEUSLER ALLOYS

- The $L2_1$ Heusler alloys with stoichiometric composition X_2YZ are in general ferromagnetic when they are of the form Co_2YZ or X_2MnZ .
- Here X is usually a transition or noble metal such as Cu, Pd, Ni; Y is a transition element such as Ti, Zr, Hf, V, Nb, and Z is an sp element belonging to groups IIIA-VA.
- In the alloys Co_2YZ the local moment is carried by the cobalt atoms and values ranging from 0.3 to 1.0 μ_B are commonly found.
- In the alloys of the form X_2MnZ the magnetic moment of about $4\mu_B$ is localized on the Mn atoms.
- The study of these alloys has made unique contribution towards the understanding of the hyperfine fields present at the impurity site in ferromagnetic metals.

- The two groups of Heusler alloys are however distinctly different from each other. In the alloys X_2MnZ the sp element at Z site is the 2nd nearest neighbour of the magnetic atom Mn. Whereas in the alloys Co_2YZ , both the sp element at Z site as well as the transition element at Y site are the nearest neighbours of the magnetic atom Co.
- Another significant difference is due to the smaller distance between the magnetic atoms in the Co based alloys.
- Heusler alloys X_2MnZ with relatively large Mn-Mn distance (≈ 1.6 times the Mn-Mn distance in pure Mn metal) constitute a class of magnetic materials half way between truly dilute systems like CuMn and concentrated systems like Fe, Co, Ni. These alloys have been studied extensively through X-ray and neutron diffraction, TDPAC, ME and NMR.

- The Heusler alloys Co_2YZ where only Co atoms have local moments and where the nearest neighbour Co-Co distance is only slightly larger (≈ 1.17 times) than in pure Co have received more attention recently because under these conditions it is quite possible that direct d-d exchange interactions play an important role in determining the magnetic properties.
- Long range magnetic coupling of localized moments via conduction electrons is however widely accepted as the dominant exchange mechanism in Heusler alloys.
- Measurement of Magnetic Hyperfine Field (mhf) acting at the magnetic and specially at non-magnetic atoms in these alloys should provide important information on conduction electron polarization (CEP) induced by the magnetic atoms on the surrounding sites.
- Such information is crucial to understanding of the mechanism which lead to magnetic ordering in Heusler alloys.

PREPARATION OF ALLOYS

- All the alloys were prepared by mixing the constituent metal powders in stiochiometric composition (except that $\approx 0.1\%$ of the Y atoms were substituted by the radioactive ^{181}Hf).
- The powders were compressed into a pellet and melted in an arc furnace under Argon atmosphere.
- After a couple of melting cycles the alloys were homogenized at $900\text{ }^{\circ}\text{C}$ for 24-72 hours and cooled slowly.
- The samples were then crushed and annealed at $800\text{ }^{\circ}\text{C}$ during 24 hours in Argon and quenched into cold water.
- Correct heat treatment for each sample was determined by X-ray analysis to obtain L2_1 structure.

TDPAC - MEASUREMENTS

- The TDPAC measurements were carried out with a conventional fast-slow coincidence setup using BaF₂ detectors having a time resolution of 0.9 ns. The well known 133-482 keV gamma cascade in ¹⁸¹Ta populated in the β^- decay of ¹⁸¹Hf was used to measure the TDPAC spectra.
- Three series of measurements were performed:
 1. Measurement at $T > T_C$ - to verify the Quadrupole interaction.
 2. Measurement at $T < T_C$ - 77 K in most cases.
 3. Measurement at $T < T_C$ - with sample polarized by a transverse external magnetic field (≈ 5 kG).

- The TDPAC Perturbation factor for an unpolarized ferromagnetic sample consisting of randomly oriented domains is given by: (neglecting the A_{44} term).

$$A_{22}G_{22}(t) = A_{22}[0.2 + 0.4\cos\omega_L t + 0.4\cos 2\omega_L t]$$

Where:

$$\omega_L = \frac{\mu_N g H_{hf}}{\hbar}$$

is the Larmor precession frequency. The g-factor of the $5/2^+$ of the 482 keV state of ^{181}Ta is known as ($g_{5/2} = 1.3$). This permits the determination of the magnitude of the ^{181}Ta mhf from the measured ω_L .

- The sign of the mhf is measured by applying an external magnetic field normal to the detector plane alternately up (\uparrow) and down (\downarrow) and measuring the ratio $R(t)$ at a fixed angle.

$$R(t, \theta = 135^\circ) = \frac{N \uparrow - N \downarrow}{N \uparrow + N \downarrow} = -0.75 A_{22} \sin 2\omega_L t$$

RESULTS

- Results of the TDPAC for some of the alloys are shown in figs. Solid curves are the least square fit of the experimental data to the theoretical expressions.
- Results of the fitting indicated that most of the alloys have unique fields with small distribution. In a few cases however it was necessary to fit the data with two distinct fields.
- This could be attributed to Ta nuclei occupying other sites within the $L2_1$ structure since the x-ray diffraction analysis did not reveal the presence of any other phase.
- It can be observed from results that Ta fields are all negative (where the signs have been measured). This is similar to that observed for non-magnetic transition element impurity in other environments like Fe, Co or Ni.
- To further illustrate this point we show in Table 1 the ratio of Ta fields to Tc and to the magnetic moment on Cobalt μ_{Co} .

- $H_{\text{Ta}}/T_c \cong 0.6\text{kOe/K}$ for $Y = \text{Sc}$
- $H_{\text{Ta}}/T_c \cong 1.1\text{kOe/K}$ for $Y = \text{Ti, Zr, Hf}$
- $H_{\text{Ta}}/T_c \cong 0.3\text{kOe/K}$ for $Y = \text{V, Nb}$

similarly

- $H_{\text{Ta}}/\mu_{\text{Co}} \cong 350\text{kOe}/\mu_{\text{B}}$ for $Y = \text{Sc}$
- $H_{\text{Ta}}/\mu_{\text{Co}} \cong 560\text{kOe}/\mu_{\text{B}}$ for $Y = \text{Ti, Zr, Hf}$
- $H_{\text{Ta}}/\mu_{\text{Co}} \cong 180\text{kOe}/\mu_{\text{B}}$ for $Y = \text{V, Nb}$
- This proportionality between H_{Ta} , T_c and μ_{Co} shows that the mhf on Ta in these alloys follow similar trends as the field on non-magnetic dilute impurities in magnetic materials such Fe, Co, Ni.
- It may be reasonable to assume that the mechanism producing the fields on Ta in the alloys Co_2YZ ($Y=\text{Sc, Ti, Zr, Hf, V, Nb}$) may also be similar.

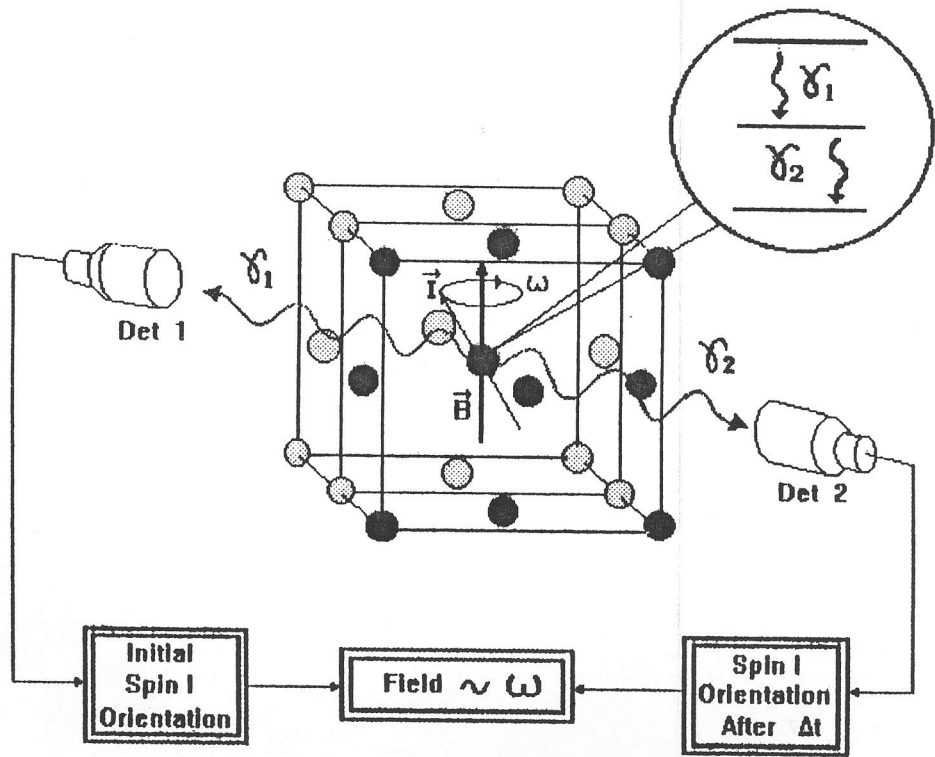
- In fact the Co-Co distance in these alloys is nearly the same as in pure Co and the impurity atom Ta is the first near neighbour in both systems.
- It is now well recognized that the reduced mhf on Sn in the alloys Co_2YSn is strongly dependent on the outer electron configuration of the Y site atom. For example $H_{\text{Sn}}/\mu_{\text{Co}}$ value increases from about $+70 \text{ kOe}/\mu_{\text{B}}$ for $Y = \text{Sc}$ to $\approx +100 \text{ kOe}/\mu_{\text{B}}$ for $Y = \text{Ti}, \text{Zr}, \text{Hf}$ and then drops rather an expectedely to $\approx +30 \text{ kOe}/\mu_{\text{B}}$ for $Y = \text{V}, \text{Nb}$.
- This is a parent contradiction with the generally observed trends where the field increases with the conduction electron density. The number of conduction electrons increase as we go from Sc to Ti to V.
- While there is no satisfactory explanation as yet for the sudden drop in the $H_{\text{Sn}}/\mu_{\text{Co}}$ value in the case of $Y=\text{V}, \text{Nb}$ it is quite clear from the present results shown in the fig. that an almost similar behavior is observed for the $H_{\text{Ta}}/\mu_{\text{Co}}$ at Y site atom in the Co_2YZ alloys
- For example $H_{\text{Ta}}/\mu_{\text{Co}}$ values are $\approx -350 \text{ kOe}/\mu_{\text{B}}$ for $Y = \text{Sc}$, $\approx -510 \text{ kOe}/\mu_{\text{B}}$ for $Y = \text{Ti}, \text{Zr}, \text{Hf}$ and $\approx -165 \text{ kOe}/\mu_{\text{B}}$ for $Y = \text{V}, \text{Nb}$.

- To summarize the results :
- Where as the reduced mhf on Ta depends strongly on the chemical nature of Y element in the Co_2YZ alloys they are rather insensitive to the chemical nature of the sp element on Z site at least within the experimental errors which come mainly from the measured values of μ_{Co} .
- The ratio $(H_{\text{Ta}}/\mu_{\text{Co}})/((H_{\text{Sn}}/\mu_{\text{Co}}))$ is approximately 5 for every pair of alloys containing the same transition element Y and this ratio is independent of the chemical group to which the element Y belongs. This suggests that the mechanism producing the the Ta and Sn fields are very similar despite a difference in the sign of the fields.
- Both $H_{\text{Ta}}/\mu_{\text{Co}}$ and $H_{\text{Sn}}/\mu_{\text{Co}}$ values seem to follow the generally observed trend of increasing field with increasing conduction electron density when for example a group IIIB element Sc at Y site is substituted by a group IVB element Ti, Zr or Hf with higher number of d-electrons.

- The behavior of V and Nb is anomalous in this respect since the reduced fields decrease when a group IVB element is replaced by a group VB element with still higher number of d-electrons.
- The reduced mhf at Ta as well as at Sn increases although slowly, within each chemical group, when outer electron configuration of the Y site element changes from 3d to 4d to 5d. This may be understood in terms of the atomic size effect which leads to higher conduction electron density for the larger atom in each group probably due to a better de-localization of the outer shell electrons.

CONCLUSIONS

- The main conclusion of the work is that the reduced mhf either on the non-magnetic transition element site or on the sp element Sn in the Co_2YZ Heusler alloy depend mainly on the chemical nature of the non-magnetic transition element Y rather than any other factor e.g. local moment μ_{Co} of the alloys, lattice parameter etc..
- The behavior of fields in alloys containing V or Nb at Y atom site is anomalous and can not be understood easily in terms of net conduction electron spin polarization at the probe nucleus.



THEORETICAL CALCULATIONS

- Theoretical calculations of the magnetic hyperfine field at the non-magnetic atom site in the Heusler alloys have been made in the past by using models of Jena and Geldart (JG) and Blandin and Campbell (BC)
- In particular these models were used to explain the systematic behavior of Sn fields, measured at Z site in the alloys of the type X_2MnZ .
- The theoretical predictions have been used to investigate the hyperfine fields in two situations: 1) in a series of alloys of the form X_2MnZ ($X = Ni, Pd, Cu$) where the Sn field increases with increasing conduction electron density and 2) in cobalt based Heusler alloys of the form Co_2MnZ and Co_2YZ , where the Sn field has been found to decrease with increasing conduction electron density.
- The behavior of the Sn field in first series of alloys has been explained well by the conduction electron polarization model of JG.

- In the case of cobalt based Heusler alloys on the other hand the JG model predictions completely disagree with the experimental values of the hyperfine fields whereas the BC theory provided a reasonable agreement with the experimental results in some cases.
- No attempts have been made in the past to predict theoretically the behavior of Y site hyperfine fields in the alloys of the form Co_2YZ largely because of the lack of experimental results.

Blandin and Campbell Model

- In the BC model the Heusler alloy is considered to be a non-magnetic host with magnetic as well as non-magnetic impurities.
- The interaction between the electrons from the conduction band of the host and the electrons from the magnetic ions induces an oscillation on the conduction electron density which is scattered by the non-magnetic impurity potential producing a net spin density on the non-magnetic site.
- The polarization $p(r_i)$ of the conduction band at a particular probe site due to a unit magnetic moment located at r_i is calculated by using an extension of the Ruderman-Kittel-Kasuya-Yosida (RKKY) interaction which takes into account perturbations in the conduction electron density resulting from localized charge at the probe atom as:

$$p(r_i) = \frac{1}{r_i^3} \cos(2k_F r_i + 2\delta_0 + \eta)$$

where k_F is the free electron Fermi vector given in terms of the average number of conduction electrons per atom n_0 as:

$$k_F = \frac{1}{a} (48\pi^2 n_0)^{1/3}$$

where a is the lattice parameter. The term δ_0 is a phase shift which accounts for the perturbation of the conduction electron density due to the effective charge of the probe atom and is given by:

$$\delta_0 = \frac{\pi}{4}(Z - n_0)$$

where Z is the probe valence. The term η is a preasymptotic correction factor.

- The hyperfine field at the non-magnetic impurity site is expressed as a sum of the partial contributions from the neighboring magnetic moments as:

$$H = A \sum_i \mu(r_i) p(r_i)$$

where A is the hyperfine coupling constant and μ is the magnetic moment of an atom located at r_i . The sum is taken over all the magnetic neighbors.

- We will describe some of the salient features of the theoretical calculations of the hyperfine fields at ^{181}Ta probe on the Y site in the Heusler alloys Co_2YZ .
- We will focus our attention on the general trends observed in a series of alloys with Y elements belonging to different chemical groups rather than comparing the precise values of mhf for single systems.

- The average number of conduction electrons per atom for Co_2YZ type of Heusler alloys can be calculated from the expression:

$$n_0 = \frac{1}{4}[2(L_{\text{Co}} - 2N_{\downarrow\text{Co}} + \mu_{\text{Co}}) + N_Y + N_Z]$$

where L_{Co} is the number of outer shell Co electrons, $N_{\downarrow\text{Co}}$ is the number of spin down Co electrons, μ_{Co} is the magnetic moment localized on Co atom and N_Y and N_Z are the number of electrons contributed to the conduction band by the Y atom and Z atom respectively.

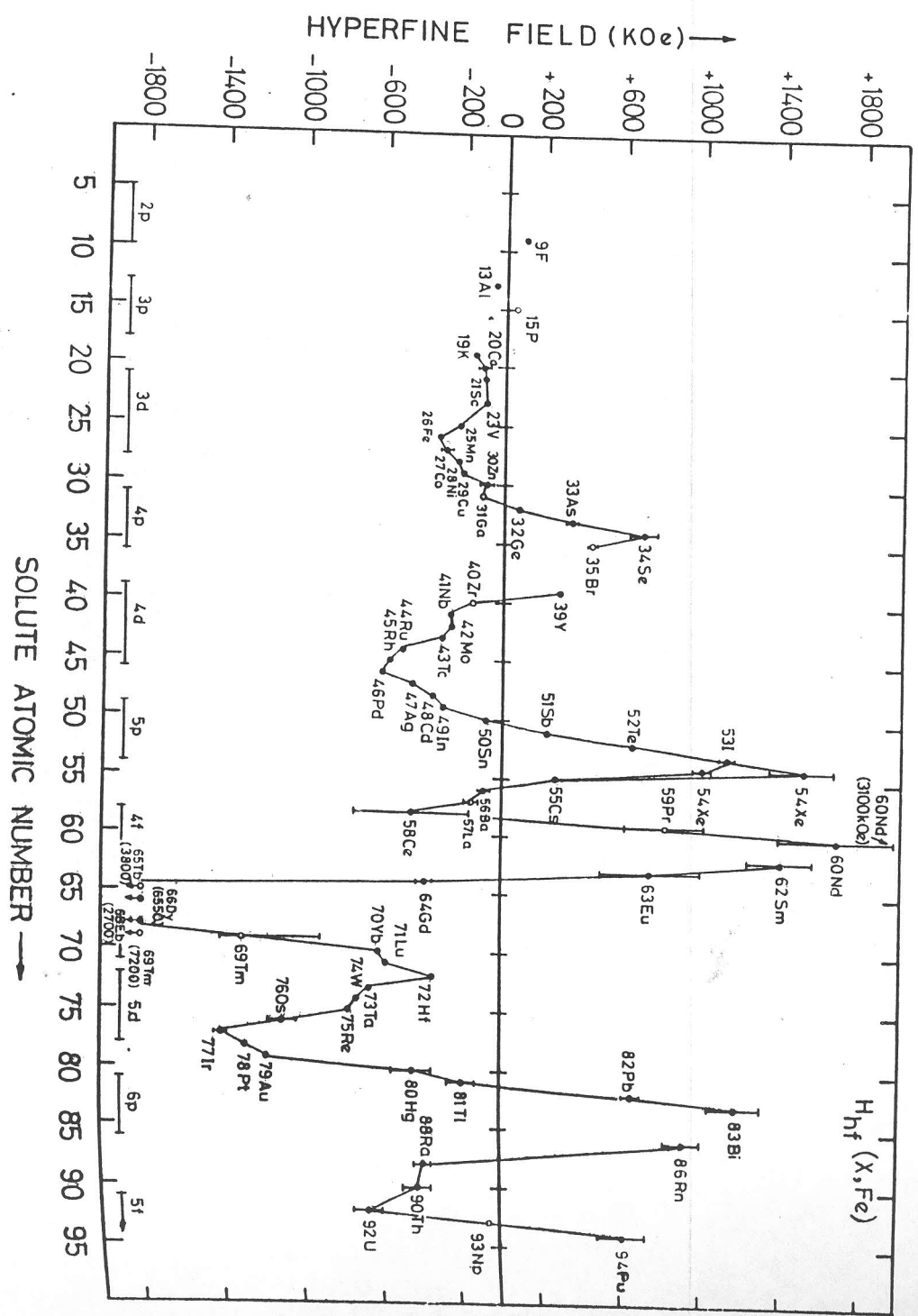
- Assigning values to N_Y and N_Z has been some what empirical in the past. It is believed however that the value of N_Z should be assumed to be the same as its chemical valence.
- The preasymptotic factor η has usually been taken as $\pi/2$ for Z site atoms which are 2nn of the magnetic ion in the Mn-based Heusler alloys.
- It has been suggested by some authors that for alloys of the type Co_2YZ ($Y \neq \text{Mn}$) the phase shift should be taken as π for 2nn in order to explain the observed trends in the Z site fields measured with ^{119}Sn and ^{111}Cd probes.

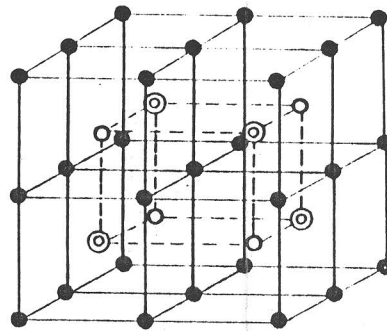
- We feel however that the choice of η in Heusler alloys X_2YZ should be made so that one gets the correct sign of the field at a given probe site.
- Using n_o and η as parameters, we have calculated the polarization $p(r_{1nn})$ for ^{181}Ta probe ($Z=5$) at Y site in the Heusler alloys Co_2YZ . The values of n_o relevant to the Heusler alloys of this type were taken in the range 0.5 to 2.0 . For a given n_o , η is initialized in the range 0 to π and polarization calculated at 1nn distance from Co atom.
- The polarization was calculated as a function of η for four different values of n_o and two different 1nn distances corresponding approximately to the largest (Co_2ZrSn) and smallest (Co_2TiSi) lattice parameters of the alloys under investigation.
- we find that in order to be able to cover simultaneously the expected range of n_o values, the polarization can be negative only for a rather limited narrow range of η values.
- In order to further narrow down the choice of η we have plotted in fig. 4 the polarization $p(r_{1nn})$ as a function of n_o for $\eta = 0, \pi/2$ and π . It can be seen that for the n_o values limited to the range 0.5 to 2.0 the most appropriate choice is $\eta = 0$ where polarization is negative.

- The conduction electron polarization as a function of n_0 for some of the Heusler alloys was calculated. Magnetic neighbors out to 8nn were considered in the summation.
- Since the aim was not to reproduce the individual hyperfine field values but to analyze the general behavior of the field as a function of the chemical nature of the Y element, it was possible to obtain a set of n_0 values for these alloys which would give a reasonable correlation between the calculated hyperfine field values and those observed experimentally.
- It is expected that this set would be consistent with the generally accepted idea that the conduction electron density increases gradually as the Y element changes progressively from group IIIB to group VIB.
- Since the variation of the Z site elements do not appreciably modify the hyperfine fields, the experimental values of the reduced fields as well as the calculated polarizations were averaged for alloys containing the same Y but different Z elements.
- The results are presented in table III along with the average values of n_0 , k_F and δ_0 .

- The hyperfine coupling constant A representing the strength of the coupling between the conduction electrons and nuclei is difficult to calculate. Usually the atomic hyperfine coupling parameter are used where they exist.
- For a given impurity probe the coupling parameter A is however constant and should not be relevant in the present context.
- It can be seen that the correlation between the experimental and theoretical results is reasonably good.
- It should be emphasized at this point that the general form of theoretically predicted behavior is sensitive only to the range of n_0 values, which are different for each chemical group to which Y element belongs, rather than the precise values for each individual alloy.
- Although RKKY mechanism is based on the assumption that the spin coupling is made essentially between the localized d-electrons (d_l) of the magnetic ion and the s-like electrons of the conduction band, it is known that a similar coupling may be possible with itinerant d-like conduction electrons also at 1nn distance and beyond.

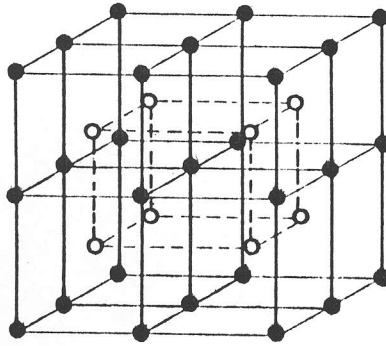
- This could explain the observed fact that the mhf at ^{181}Ta increases gradually within each chemical group, when the outer electron configuration of the Y site element changes from 3d to 4d to 5d.
- This reflects an atomic size effect which leads to a higher d-contribution to the conduction electron density for larger atoms in the same group presumably due to a better delocalization of the outer shell electrons.
- An examination of the data shows that, in every series of alloys containing a given Z element, the value of the local magnetic moment decreases somewhat as the outer electron configuration of Y element changes from 3d to 4d to 5d.
- This indicates that number of electrons which contribute to form the magnetic moment decreases and, as a consequence, the contribution to the conduction electron band increases in going down the group.





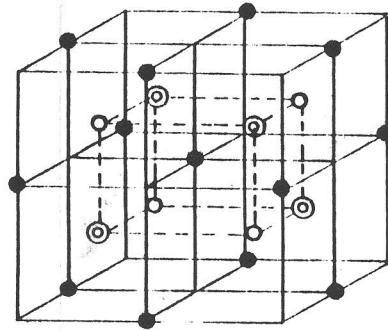
$L2_1$
 X_2YZ

● X
⊙ Y
○ Z



B2
 X_2YZ

● X
○ Y, Z



$C1_b$
 XYZ

● X
⊙ Y
○ Z

Figura II.1: Estruturas possíveis para as ligas de Heusler

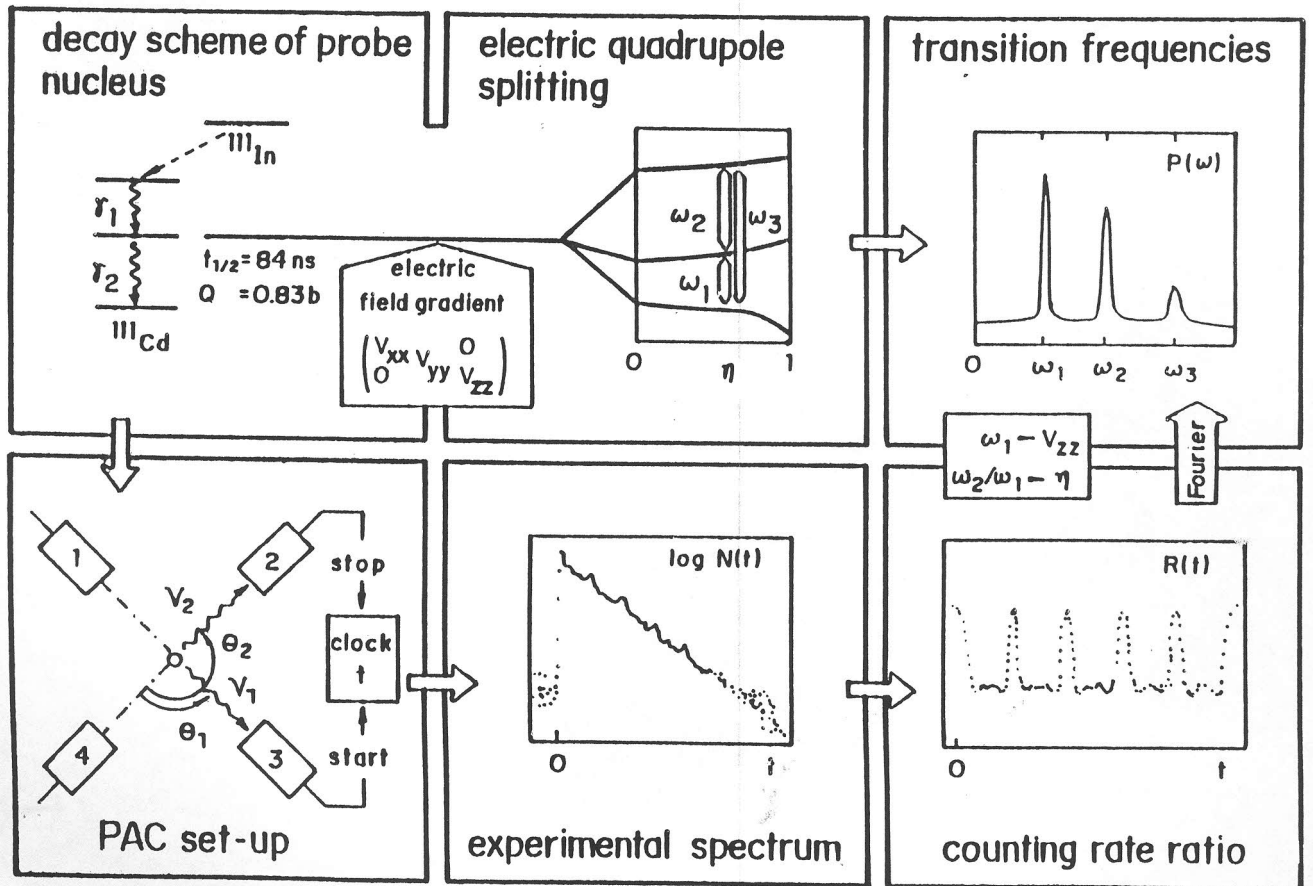


Figura 4: Esquema do Método de Correlação Angular Perturbada

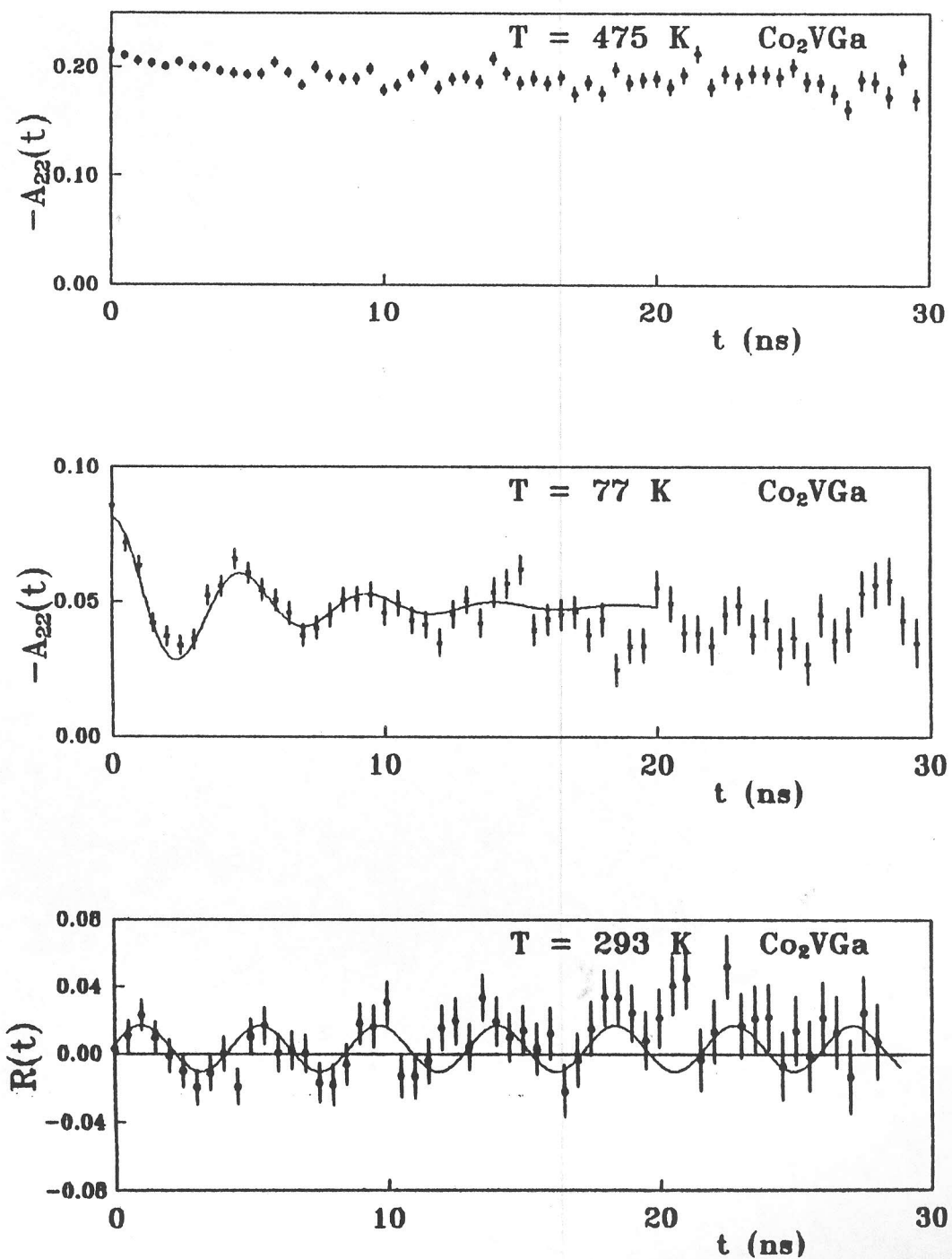


Figura VI.4: Curvas de $A_{22}(t)$ e $R(t)$ para a liga Co_2VGa

também é negativo.

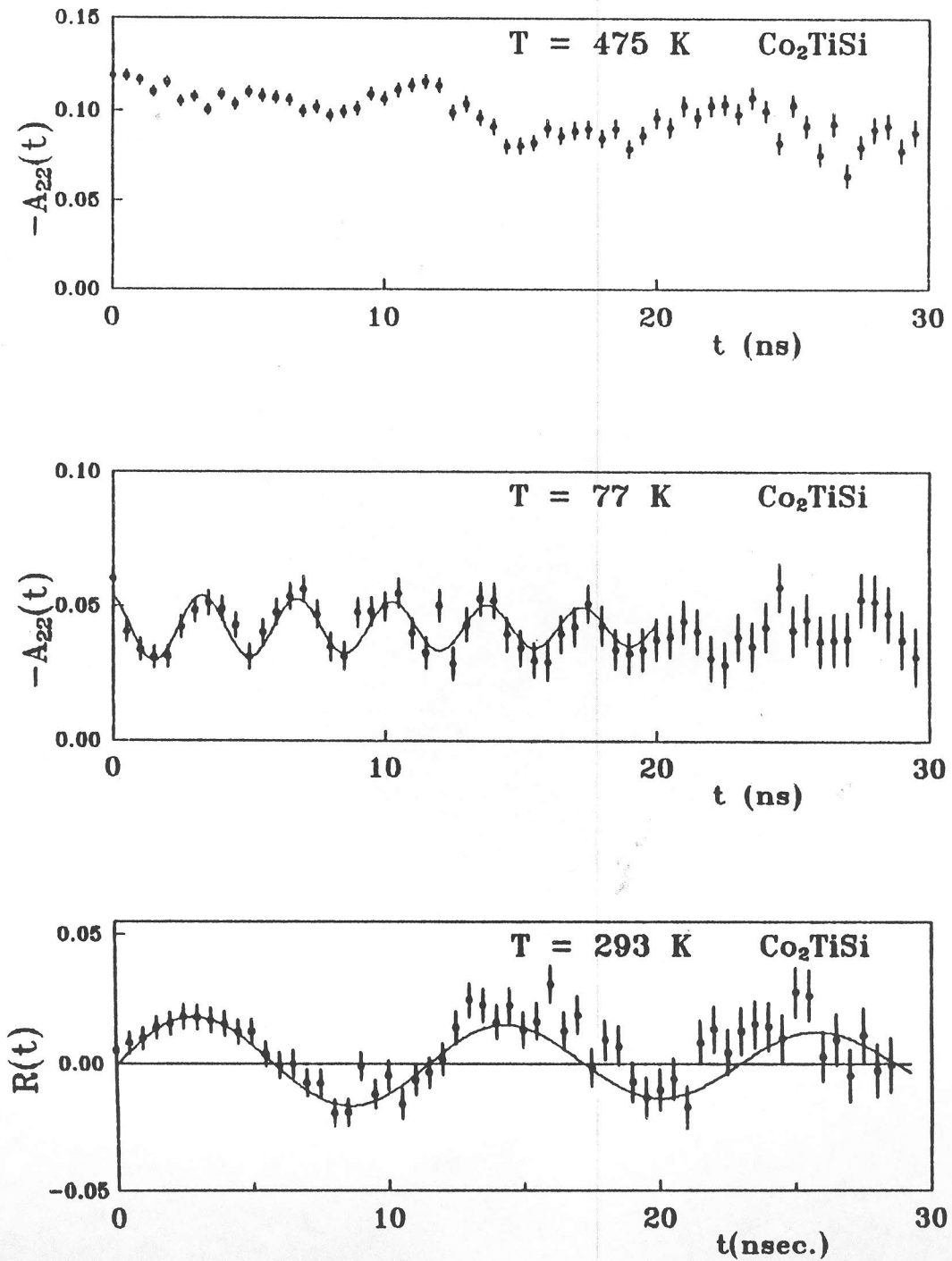


Figura VI.5: Curvas de $\Lambda_{22}(t)$ e $R(t)$ para a liga Co_2TiSi

6.2.5. Liga Co_2VSn

Como esta liga possui uma temperatura de Curie muito baixa (95 K), a fase paramagnética foi medida à temperatura ambiente (293 K) e a fase ferromagnética foi medida na temperatura

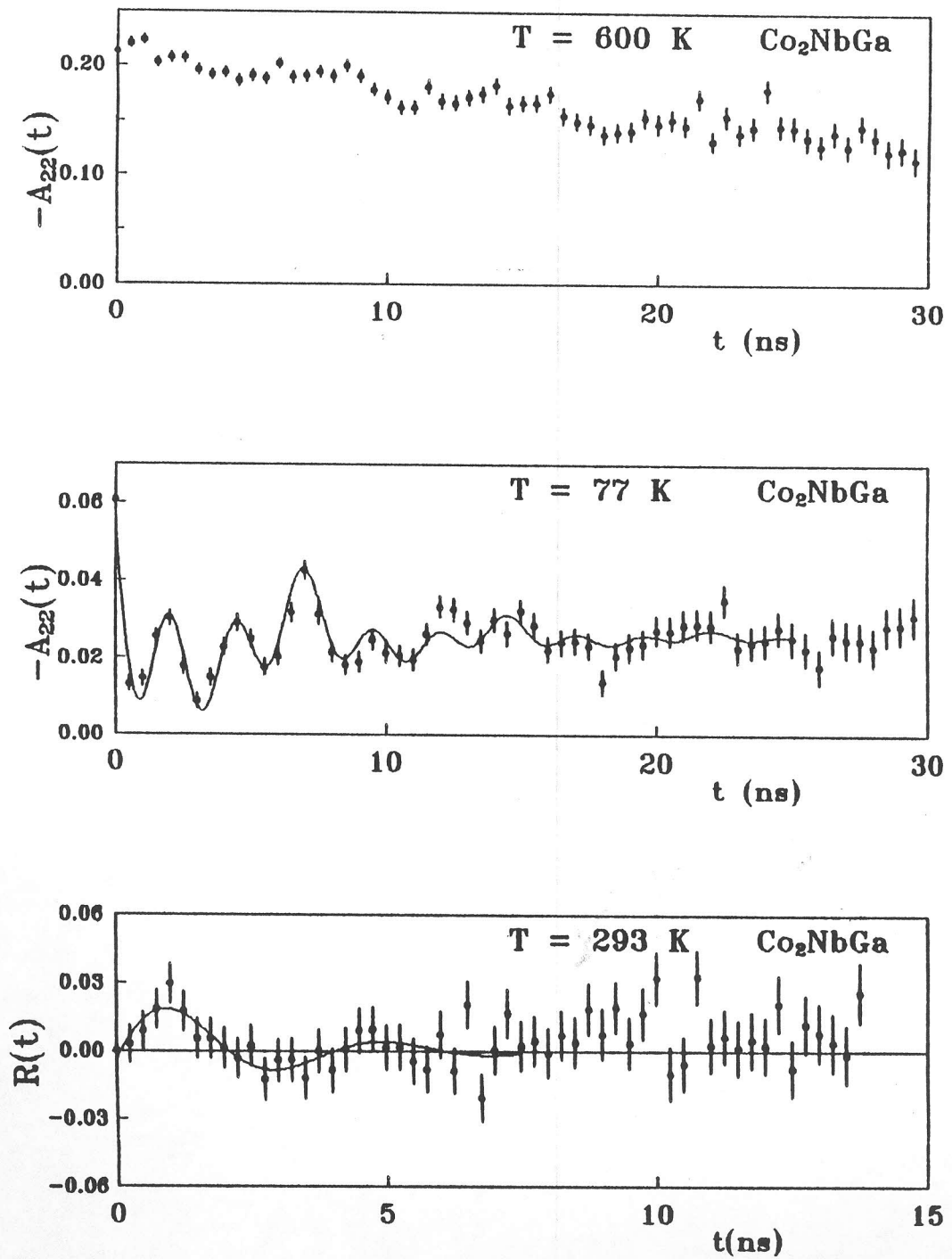
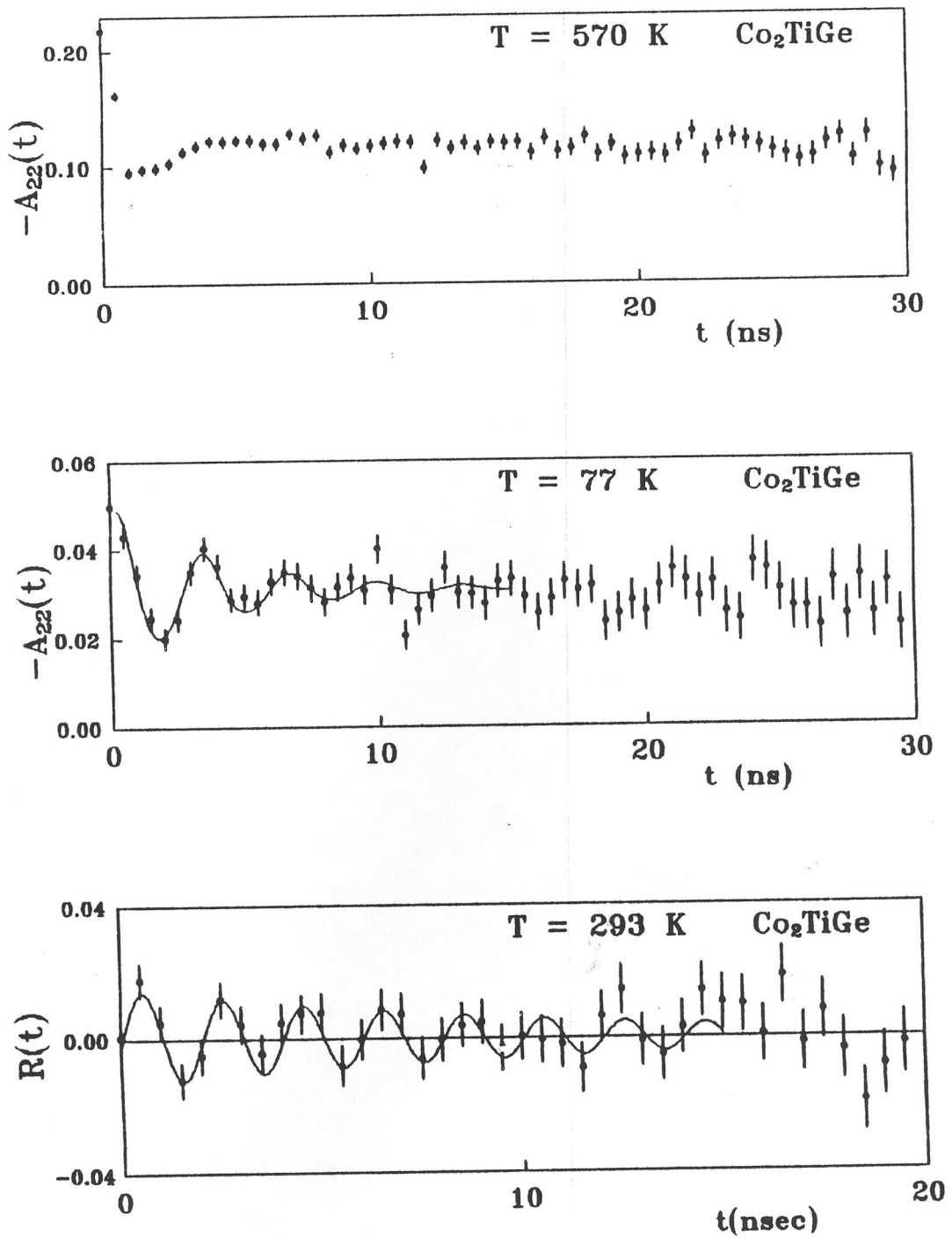


Figura VI.3: Curvas de $A_{22}(t)$ e $R(t)$ para a liga Co_2NbGa

A curva de $R(t)$, também mostrada na figura VI.4, indica que o sinal do CHM neste caso

Figura VI.6: Curva de $A_{22}(t)$ e $R(t)$ para a liga Co_2TiGe

do nitrogênio líquido (77 K). Não foi possível realizar a medida para a verificação do sinal

Table: Magnetic properties of the Co₂YZ Heusler alloys.

alloy	a ₀ (Å)	T _c (K)	μ _{Co} (μ _B)	H _{Ta} (77K) (kOe)	H _{Ta} /μ _{Co} (kOe/μ _B)	H _{Sn} /μ _{Co} (kOe/μ _B)
Co ₂ ScGa	6.17		0.25	(-)90(2)	(-)360	
Co ₂ ScGe	5.78		0.55	-209(2)	-380	
Co ₂ ScSn	6.19	268	0.55	-187(3)	-341	+73(13)
Co ₂ TiAl	5.85	138	0.35	-143(4)	-409	
Co ₂ TiGa	5.85	130	0.40	(-)159(4)	(-)398	
Co ₂ TiSi	5.74	375(4)	0.55	-287(6)	-522	
Co ₂ TiGe	5.83	386(4)	0.89	-312(6)	-351	
Co ₂ TiSn	6.07	371	1.03	(-)480(6)	(-)466	+81(8)
Co ₂ ZrAl	6.08	178	0.30	-184(4)	-613	
Co ₂ ZrSn	6.25	448	0.80	(-)380(6)	(-)475	+110(14)
Co ₂ HfAl	6.02	193	0.40	-189(4)	-473	
Co ₂ HfGa	6.03	186	0.30	-213(4)	-710	
Co ₂ HfSn	6.22	396	0.77	-421(12)	-547	+138(18)
Co ₂ VAl	5.80	310(4)	0.92	-116(4)	-126	
Co ₂ VGa	5.78	352	1.05	(-)218(6)	-208	
Co ₂ VSn	5.98	105	0.60	(-)108(2)	(-)180	+12(3)
Co ₂ NbAl	5.94	383	0.67	-138(4)	-206	
Co ₂ NbGa	5.95	-	0.70	-135(2)	-193	
Co ₂ NbSn	6.15	105	0.26			+58(15)
Co ₂ TaAl	5.93	260	0.75	-156(7)	-208	
Co ₂ CrAl	5.89	334	0.78	-124(5)	-159	